Flexural Behavior of High Volume Fly Ash-Self Compacting Concrete Beams to Normal Concrete Beams with Conventional Steel Reinforcement

Rosyid Kholilur Rohman
Civil Engineering Department, Merdeka University of Madiun, East Java, Indonesia
rosyid@unmer-madiun.ac.id (corresponding author)

Rendi Gusta Wibowo
Civil Engineering Department, Merdeka University of Madiun, East Java, Indonesia
rendigusta@unmer-madiun.ac.id

Arif Afrianto
Civil Engineering Department, Merdeka University of Madiun, East Java, Indonesia
arifafrianto@unmer-madiun.ac.id

Received: 19 August 2024 | Revised: 22 August 2024 | Accepted: 22 September 2024

 DOI: https://doi.org/10.48084/etasr.8771

ABSTRACT

This research determines the comparison between the flexural behavior of Normal Concrete (NC) beams and High-Volume Fly Ash Self Compacting Concrete (HVFA-SCC) beams. The research data was obtained from full-scale beam tests using four-point loading. Tests were carried out on 6 NC and 6 HVFA-SCC beam specimens with dimensions of 150 mm × 250 mm × 2000 mm. The test specimens varied with main reinforcement of 12 mm, 16 mm, and 19 mm diameter. The results of the studies show that the crack patterns of the NC and HVFA-SCC beams are almost identical to those of the flexural failure mode, while the HVFA-SCC beam has greater ductility than the NC beam. The nominal flexural strength (Mn) of HVFA-SCC beams can be calculated using the Mn formula in ACI 318-19.

Keywords-displacement; ductility; nominal flexural strength; HVFA-SCC

I. INTRODUCTION

The use of Fly Ash (FA) as a partial replacement of cement in concrete work is a solution to reduce environmental problems caused by energy consumption in cement production [1, 2]. At present, the production of 1.0 kg of cement produces 0.9 kg of CO_2 emissions [3]. Replacing part of the cement with FA in concrete production is one solution to reduce greenhouse gas emissions. Several studies have shown that it is possible to use FA on a large scale. The proportion of partial cement replacement with fly ash of at least 50% is high volume fly ash concrete [4, 5]. The use of FA, which is a coal combustion waste, also reduces the environmental impact of landfill disposal.

One of the problems with reinforced concrete is the limited space for the fresh concrete to move due to the presence of the reinforcement. The fresh concrete mix cannot reach small gaps in the formwork, even when a vibrator is used. The use of Self-Compacting Concrete (SCC) can overcome this problem. SCC can compact itself, fill the mold cavity and pass through the reinforcement without vibration [6-8]. This feature is achieved through the use of a Superplasticizer (SP) and finer aggregate proportions compared to normal concrete (NC), which ensures that the flowability of SCC is high. Combining the HVFA and SCC concepts is an attempt to achieve sustainable concrete in the future [9]. The effect of the FA addition on the flexural behavior of reinforced concrete beams has been examined by researchers. Bending tests were conducted on reinforced concrete beams with FA contents ranging from 0% to 60% and a water-cement ratio of 0.4. The experimental findings indicate that the maximum load of beams containing 30% FA is the largest of all beams [10]. The flexural strength of a reinforced concrete beam incorporating FA is observed to be marginally higher than that of a control beam, with an enhanced proportion of 6.37% [11]. The behavior of HVFA concrete beams has been the subject of research, which has involved a comparison of the results of beam bending tests. The present study compares the bending behavior of NC beams and HVFA

beams. The findings of this study indicate that the HVFA concrete beam exhibits a flexural capacity that is comparable to that of the NC beam [12]. Other research indicates that beams containing 30% and 50% fly ash exhibit flexural behavior comparable to that of the control beam specimen, which was not replaced with alternative cementitious materials [13]. The SCC beam specimens were manufactured using a water-powder ratio of 0.4 and a SP content of 1.25% of the cement weight. The concrete beam specimens, measuring 100 mm × 200 mm, had a length of 1,200 mm. The beam flexural test was carried out with two-point loads. The results of this research demonstrate that the beams exhibited flexural failure modes. Consequently, the SCC beam demonstrated superior performance to the NC beam in terms of flexural capacity [7].

Further research is required to gain a deeper understanding of the flexural behavior of HVFA-SCC beams. Authors in [14] conducted research into the flexural behavior of HVFA-SCC slabs. This research examined the differences in flexural behavior between NC and HVFA-SCC slabs with GFRP reinforcement. The findings of the research demonstrate that HVFA-SCC slabs reinforced with GFRP exhibit comparable structural behavior to NC slabs with GFRP reinforcement. Authors in [15] indicate that the discrepancy in ultimate bending moment between OPC and HVFAC beams is within 7% in the two groups of beams tested, while authors in [16] present evidence that the tension stiffening stress on the HVFA-SCC beam is greater than on the NC beam. The present study compares the behavior of HVFA-SCC and NC beams with conventional steel reinforcement. The analysis encompassed an examination of the failure modes, crack patterns, cracking moments, and capacity moments. Subsequently, the experimental and analytical results in accordance with the ACI 318-19 design standard will be compared.

II. EXPERIMENTAL WORK

A. Materials

The Coarse Aggregate (CA) used is crushed stone, whereas the fine aggregate employs river sand and is categorized within grading zone 2. The maximum coarse aggregate size is 20 mm. The coarse and fine aggregates were sourced from PT. Varia Usaha Beton Karanganyar, Central Java, Indonesia. Prior to their usage in the fabrication of test specimens, both aggregates underwent evaluation in a material laboratory to ascertain their conformity with the SNI requirements for incorporation into concrete mixtures. The aggregate test outcomes are presented in Table I.

TABLE I. AGGREGATE TEST RESULTS

Material	Weight per volume (kg/m^3)	Specific Gravity (kg/m^3)	Fineness Modulus	Mud content (%)	Absorption (%)
Coarse aggregate	1,417	2.65	7.63	0.78	2.22
Fine Aggregate	1,541	2.53	2.96	3.54	3.54

The FA used in this research was provided by PLTU Tanjung Jati Jepara and contains 43.82% SiO_2, 15.58% Al_2O_3, and 12.13% FeO, resulting in a total of 71.53%. It appears that the FA in question is of the C type. Moreover, a SP is added to enable the concrete to solidify autonomously, which is Consol P 292 AS, produced by PT Kimia Beton Indonesia. A series of tests were performed on the trial mix in order to ascertain a compressive strength of 30 MPa. Furthermore, tests were conducted during the trial mix to ensure that the resulting concrete would meet the requirements for SCC. The resulting mix design is presented in Table II.

TABLE II. MIX DESIGN OF NC AND HVFA-SCC

Material	Cement (kg/m^3)	FA (kg/m^3)	CA (kg/m^3)	Fine aggregate (kg/m^3)	SP (kg/m^3)	Water (kg/m^3)
NC	450	-	940	870	-	180
HVFA-SCC	275	275	876	635	5.5	176

The process of creating a test specimen commences with the weighing of the concrete constituent materials in accordance with the outcomes of the trial mix. The process of mixing the concrete ingredients initially involves the incorporation of the cement, FA, and aggregates into the mixer. The requisite volume of water is then added, amounting to three-quarters of the total required. Subsequently, a quarter of the requisite volume of water is added, followed by the incorporation of the SP into the mixer. The mixing process was completed in approximately five minutes, during which it was observed that the resulting concrete mixture exhibited a homogeneous, brownish coloration. To guarantee that the concrete mixture fulfils the requirements of SCC, tests are performed on the fresh concrete. In accordance with the EFNARC 2005 standard, the slump flow, V-funnel, and L-box tests are necessary to be carried out. It is essential to ensure the flowability of the concrete mixture in order to meet the requisite characteristics of SCC. The results of the slump flow test are presented in Table III, while the test itself is shown in Figure 1.

TABLE III. THE RESULT OF THE FRESH CONCRETE TEST

Test	Test result	Unit	Requirement	Conclusion
Slump flow	670	mm	650 - 800	OK
V funnel	9.10	sec	6 - 12	OK
L Box	0.86	mm/mm	0.8 – 1.0	OK
T 50	4.50	sec	2 - 5	OK

Concrete compressive strength testing is a method of evaluating the quality of concrete. The test object is a concrete cylinder with a height of 300 mm and a diameter of 150 mm, in accordance with the specifications set forth in ASTM C39. Subsequently, the concrete cylinder mold is removed on the following day, after which the specimen is treated by immersion in water. Prior to the commencement of the compression test, the specimen is subjected to a drying process and subsequently weighed in order to determine its volume weight. The test was conducted using compressive strength apparatus with a limit of 2000 kN at a specimen age of 28 days. The test is performed by applying a compressive force to the concrete cylinder until it is crushed. The resulting compressive force is obtained from the manometer reading of the compressive strength equipment. The compressive strength is

calculated by dividing the compressive force by the cross-sectional area of the specimen. The results of the compressive strength test are presented in Table IV.

Fig. 1. Slump flow test.

TABLE IV. COMPRESSIVE STRENGTH TEST

Specimen	Volume weight (kg/m^3)	Compressive strength (MPa)	Average compressive strength (MPa)
NC	2,318	31.99	31.80
	2,266	30.86	
	2,312	32.55	
HVFA-SCC	2,319	33.40	33.12
	2,328	32.27	
	2,308	33.69	

A tensile test was applied to the steel reinforcement using a Universal Testing Machine (UTM) with a capacity of 1000 kN. The test standard is in accordance with ASTM A-370-03a. The objective of the test is to ascertain the ability of the reinforcement to withstand stress, defined as the force per unit area. The results of the test will enable the determination of the maximum tensile strength, which is presented in Table V.

TABLE V. STEEL REINFORCEMENT TEST

Diameter (mm)	Effective diameter (mm)	Yield strength (MPa)	Ultimate strength (MPa)
8	7.7	340	470
12	11.6	420	587
16	15.6	415	582
19	18.7	403	560

B. Beam Specimens

This research is based on an experimental methodology. The experiment was conducted using beam specimens with dimensions of 150 mm in width, 250 mm in height, and 2,000 mm in length. Tensile reinforcement is provided by deformed bars with diameters of 12 mm, 16 mm, and 19 mm. The stirrups and compressive reinforcement use plain steel rods with an 8 mm diameter and the concrete cover has a thickness of 25 mm. In all test specimens, stirrups were installed at one-third of the span on the left and right edges, with a spacing of 70 mm. The objective of installing the stirrups is to prevent shear failure during beam testing. Two distinct types of beam specimens were created, as presented in Table VI. For each specimen type, two test beams were constructed, resulting in a total of 12 beams for testing. A diagram of the beam specimen for tensile reinforcement D16 is shown in Figure 2.

TABLE VI. BEAM SPECIMENS

Specimen	$f'c$ (MPa)	fy (MPa)	b (mm)	h (mm)	d_b (mm)
NC 12	31.80	420	150	250	11.6
NC 16	31.80	415	150	250	15.6
NC 19	31.80	403	150	250	18.7
HVFA-SCC 12	33.12	420	150	250	11.6
HVFA-SCC 16	33.12	415	150	250	15.6
HVFA-SCC 19	33.12	403	150	250	18.7

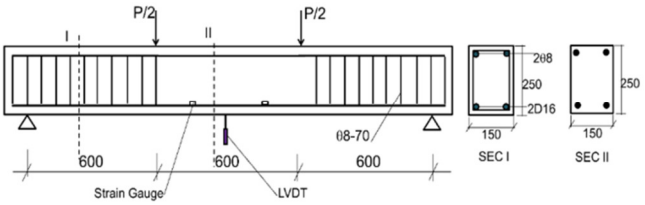

Fig. 2. Beam specimen sketch (D16).

C. Beam Testing Setup

The configuration of the beam testing apparatus is shown in Figure 3.

Fig. 3. Setup of beam specimen.

The beam is subjected to a four-point load in order to carry out the necessary testing. The working concentrated load is distributed to the beam via the load distribution beam. It was determined that the distance between the two-point loads should be 600 mm. The distance between the centralized load and the nearest placement is 600 mm. The beam is supported by means of a steel pedestal. The load is quantified by a load cell situated in the center of the load distribution beam. A strain

gauge is installed and connected to a strain indicator at the mid-span tensile reinforcement. The strain value of the reinforcing steel can be ascertained from the reading displayed on the strain indicator. LVDTs are installed on either side of the beam in order to ascertain the extent of any deflection that may occur. The occurrence of cracks is indicated on the surface of the beam specimen at each loading interval of 5 kN.

III. RESULTS AND DISCUSSION

A. Failure Modes and Crack Patterns

Figures 4 and 5 show the crack patterns observed in the NC and HVFA-SCC beams, respectively. The cracks that emerge are of a flexural nature and oriented vertically. The initial fracture occurs in the mid-span region, which is subject to constant moment loading. This area is subjected to greater tensile stress as a result of the applied load. Furthermore, additional flexural cracks are formed between the two loads and emplacements. As the load increases, the vertical cracks progressively extend into the compression zone. In the beam specimen, the applied load resulted in the tensile reinforcement yielding, which was subsequently followed by the concrete breaking in the compression area. The beam specimen demonstrated ductility, and no sudden collapse occurred. The test results demonstrate that the failure of HVFA-SCC and NC beams is flexural. The absence of shear cracks in the specimen indicates that shear failure did not occur. The observation results demonstrate that the crack patterns in NC and HVFA-SCC beams are essentially identical.

Fig. 4. NC beam crack pattern.

Fig. 5. HVFA-SCC beam crack pattern.

B. Load vs. Displacement

In this test, the formation of cracks in the beam's cross-section is documented, with a particular focus on three crucial structural behaviors that are employed to assess the value of the beam's flexural capacity. This behavior includes an examination of the concrete's condition at the point of initial cracking, the point of yielding, and the ultimate condition. Figure 6 shows the relationship between load and displacement for each beam. The graph demonstrates the response of a beam to flexural loading, with each beam exhibiting a similar pattern, namely the formation of a trilinear curve. An increase in load will result in a corresponding increase in displacement. From the moment the load is applied until the initial cracking of the beam occurs, the curve represents the first linear relationship between load and displacement. Subsequent to the load at the time of the primary fracture, the curve will undergo a reversal, exhibiting a second linear relationship between load and displacement until the steel reinforcement reaches its yield stress. The application of this load enables the beam to maintain its relatively high stiffness. Upon reaching the limit of the second linear curve, a third linear relationship becomes evident, whereby a slight increase in load results in a notable rise in displacement value. This indicates that the beam has reached a plastic state, whereby its stiffness has been significantly diminished until the point of failure. Following the yield point of the reinforcement, the deflection graph for NC and HVFA-SCC concrete exhibits no discernible difference. Nevertheless, the maximum deflection value observed in the HVFA-SCC beam is greater than that observed in the NC beam. This demonstrates that the incorporation of FA can enhance the ductility of HVFA-SCC beams.

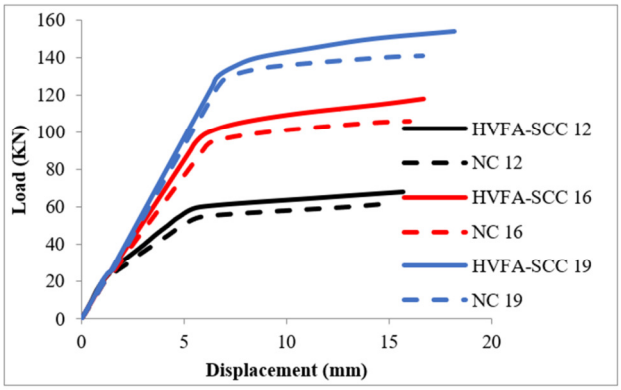

Fig. 6. Load vs. displacement.

From this figure, an analysis of the displacement ductility of the beam specimen can be performed. The displacement ductility is defined as the ratio between the ultimate displacement and the displacement at the time of yielding:

$$\mu = \frac{\delta u}{\delta y} \quad (1)$$

where μ, δu, δy are the ductility displacement, maximum structural deflection, and deflection when yielding occurs, respectively. The results of the displacement ductility calculations are presented in Table VII. HVFA-SCC beams display greater ductility than NC beams. In specimens of varying diameter (12 mm, 16 mm, and 19 mm), there is a notable discrepancy in displacement ductility, with values differing by 7.20%, 7.74%, and 6.36%, respectively, in comparison to the NC group. The mean discrepancy in displacement ductility is 7.10%.

TABLE VII. DISPLACEMENT DUCTILITY OF NC AND HVFA-SCC BEAMS

Code	Yield displacement (mm)	Max. displacement (mm)	Displacement Ductility
NC 12	6.00	15.15	2.53
NC 16	6.40	16.00	2.50
NC 19	7.20	16.65	2.31
HVFA-SCC 12	5.80	15.70	2.71
HVFA-SCC 16	6.20	16.70	2.69
HVFA-SCC 19	7.40	18.20	2.46

C. Cracking Moment and Nominal Flexural Strength

The cracking moment (M_{cr}) is defined as the moment value at which the initial crack formation occurs as a result of the applied loading [17]. This moment is triggered when the tensile stress within an element surpasses the tensile strength of the material, leading to the formation of cracks. The cracking moment is a significant factor in the design of concrete structures. The value of the M_{cr} can be calculated:

$$M_{cr} = \frac{f_r \cdot I_g}{y_t} \quad (2)$$

$$f_r = 0.62\sqrt{f'_c} \quad (3)$$

where f_r is the modulus of rupture, I_g is the gross moment of inertia, y_t is the neutral line of the concrete beam specimens, and $f'c$ is the concrete´s compressive strength. The nominal flexural strength is defined as the moment of cross-sectional analysis based on the principles of static equilibrium and compatibility of stress and strain. The tensile force in the steel reinforcement and the compressive force in the concrete act in opposition to one another in order to resist this moment. The nominal flexural strength (M_n) of the reinforced concrete beam can be calculated:

$$M_n = \rho f_y b d^2 \left(1 - 0.59\rho \frac{fy}{f'_c}\right) \quad (4)$$

Table VIII presents a comparison of experimental and calculated cracking moments, while Table IX provides a comparison of flexural strength from experimental and calculated results using the ACI 318-19 formula. Table VIII shows that the cracking moment derived from the experimental data is greater than that obtained from the calculations for both the NC and HVFA-SCC beams. In the NC beam, the test results indicate a 6% greater cracking moment (M_{cr}) than the calculated values. In contrast, the HVFA-SCC beam exhibits a M_{cr} that is approximately 15% greater than the calculated values.

TABLE VIII. COMPARISON M_{CR} EXPERIMENT WITH CALCULATION RESULT ACCORDING TO ACI 318-19

Code	M_{cr} Cal. (kNm)	M_{cr} Exp. (kNm)	Exp/Cal.	Average Exp/Cal.
NC 12	6.17	6.50	1.05	1.06
NC 16	6.17	6.54	1.06	
NC 19	6.17	6.63	1.07	
HVFA-SCC 12	6.29	7.22	1.15	1.15
HVFA-SCC 16	6.29	7.25	1.15	
HVFA-SCC 19	6.29	7.35	1.17	

TABLE IX. COMPARISON M_N EXPERIMENT WITH M_N CALCULATION RESULT ACCORDING TO ACI 318-19

Code	M_n Cal. (kNm)	M_n Exp. (kNm)	Exp/Cal.	Average Exp/Cal.
NC 12	17.77	18.6	1.05	1.06
NC 16	30.06	31.8	1.06	
NC 19	39.89	42.3	1.06	
HVFA-SCC 12	17.80	20.4	1.15	1.16
HVFA-SCC 16	30.19	35.4	1.17	
HVFA-SCC 19	40.13	46.2	1.15	

Table IX indicates that the flexural strength derived from the experimental data for the NC beam is nearly identical to that predicted by the calculations. A comparison between the experimental and calculated results yields a ratio of 1.06. This result is consistent with the findings of previous research [12], which demonstrated a ratio of flexural strength between experimental and calculated results of approximately 1. Additionally, the flexural strength of HVFA-SCC beams is 1.16 times greater than the calculated value of Mn using (4). The existing ACI 318-19 design standard is excessively conservative in its estimation of the flexural strength of HVFA-SCC beams.

IV. CONCLUSIONS

The objective of this study was to investigate the flexural behavior of High-Volume Fly Ash Self Compacting Concrete (HVFA-SCC) and Normal Concrete (NC) beams with conventional reinforcement. In this research, the use of Fly Ash (FA) for HVFA-SCC beams was equivalent to 50% cement. A static two-point bending test was employed to evaluate the structural performance of the reinforced concrete beam specimens. The assessment included an analysis of the crack patterns, failure modes, deflection values due to applied loads, cracking loads, and ultimate loads. The following conclusions were drawn from the experiments conducted in this study:

- The crack patterns observed in the NC and HVFA-SCC beam specimens were found to be largely similar. The initial fracture occurs in the mid-span tensile zone. As the load increases, the crack expands beyond the region of constant moment. The crack will continue until it reaches the compression area, resulting in damage to the concrete. The failure mode observed in the HVFA-SCC and NC beam specimens is a flexural failure.
- It was observed that the ultimate load of the HVFA-SCC beam exceeded that of the NC beam. Furthermore, the displacement value is also greater. The usage of HVFA-SCC will result in the production of reinforced concrete beams with enhanced ductility. The HVFA-SCC beam displays greater ductility than the NC beam, with a difference of approximately 7.10%.
- The calculated nominal flexural strength according to the ACI 318-19 formula is found to be smaller than the nominal flexural strength derived from the experimental results. The existing ACI 318-19 design standard provides a conservative estimate of the nominal flexural strength of HVFA-SCC beams.

The findings of this study indicate that HVFA-SCC is a suitable material for use in reinforced concrete beams. The flexural performance of the HVFA-SCC beam with conventional steel reinforcements is superior to that of the NC beam. Moreover, the usage of HVFA-SCC in structural engineering projects can be contemplated in the context of environmental concerns. The application of HVFA-SCC in concrete construction will result in a 50% reduction in cement usage and a consequent reduction in greenhouse gas emissions. The findings of this study are in accordance with the research conducted by authors in [14], which indicated that the application of HVFA-SCC as an alternative to NC in engineering practice is a viable proposition.

ACKNOWLEDGEMENT

The authors thank all the lecturers and the educational staff of the Civil Engineering Study Program, Merdeka University of Madiun, who have supported this research. The publication of this research is supported by Yayasan Perguruan Tinggi Merdeka Madiun.

REFERENCES

[1] S. A. Chandio, B. A. Memon, M. Oad, F. A. Chandio, and M. U. Memon, "Effect of Fly Ash on the Compressive Strength of Green Concrete," *Engineering, Technology & Applied Science Research*, vol. 10, no. 3, pp. 5728–5731, Jun. 2020, https://doi.org/10.48084/etasr.3499.

[2] N. Bheel, M. A. Jokhio, J. A. Abbasi, H. B. Lashari, M. I. Qureshi, and A. S. Qureshi, "Rice Husk Ash and Fly Ash Effects on the Mechanical Properties of Concrete," *Engineering, Technology & Applied Science Research*, vol. 10, no. 2, pp. 5402–5405, Apr. 2020, https://doi.org/10.48084/etasr.3363.

[3] R. K. Rohman, S. A. Kristiawan, H. A. Saifullah, and A. Basuki, "The development length of tensile reinforcement embedded in High Volume Fly Ash-Self Compacting Concrete (HVFA-SCC)," *Construction and Building Materials*, vol. 348, Sep. 2022, Art. no. 128680, https://doi.org/10.1016/j.conbuildmat.2022.128680.

[4] H. H. Alghazali, Z. K. Al-Jaberi, Z. R. Aljazaeri, and J. J. Myers, "Flexural performance of extremely damaged reinforced concrete beams after SRP repair," in *Advances in Engineering Materials, Structures and Systems: Innovations, Mechanics and Applications*, CRC Press, 2019.

[5] S. A. Kristiawan, "Uniaxial Compressive Stress-Strain Behavior of Self-Compacting Concrete wuth High-Volume Fly Ash," *International Journal of Geomate*, vol. 14, no. 41, pp. 77–85, Jan. 2018, https://doi.org/10.21660/2018.41.19423.

[6] *European Guidelines for Self Compacting Concrete (SCC)*. EFCA, 2005.

[7] M. M. Seles, R. Suryanarayanan, S. S. Vivek, and G. Dhinakaran, "Study on Flexural Behaviour of Ternary Blended Reinforced Self Compacting Concrete Beam with Conventional RCC Beam," *IOP Conference Series: Earth and Environmental Science*, vol. 80, no. 1, Jul. 2017, Art. no. 012026, https://doi.org/10.1088/1755-1315/80/1/012026.

[8] M. A. Memon, N. A. Memon, A. H. Memon, R. Bhanbhro, and M. H. Lashari, "Flow Assessment of Self-Compacted Concrete incorporating Fly Ash," *Engineering, Technology & Applied Science Research*, vol. 10, no. 2, pp. 5392–5395, Apr. 2020, https://doi.org/10.48084/etasr.3283.

[9] H. H. Alghazali and J. J. Myers, "Shear behavior of full-scale high volume fly ash-self consolidating concrete (HVFA-SCC) beams," *Construction and Building Materials*, vol. 157, pp. 161–171, Dec. 2017, https://doi.org/10.1016/j.conbuildmat.2017.09.061.

[10] B. S. Raj and M. K. Rao, "Flexural Performance of Sustainable Fly Ash Based Concrete Beams," *IOP Conference Series: Earth and Environmental Science*, vol. 1130, no. 1, Jan. 2023, Art. no. 012021, https://doi.org/10.1088/1755-1315/1130/1/012021.

[11] W. N. Oktaviani, A. Tambusay, I. Komara, W. Sutrisno, F. Faimun, and P. Suprobo, "Flexural Behaviour of a Reinforced Concrete Beam Blended with Fly ash as Supplementary Material," *IOP Conference Series: Earth and Environmental Science*, vol. 506, no. 1, May 2020, Art. no. 012042, https://doi.org/10.1088/1755-1315/506/1/012042.

[12] M. Arezoumandi, C. A. Ortega, and J. S. Volz, "Flexural Behavior of High-Volume Fly Ash Concrete Beams: Experimental Study," *Transportation Research Record*, vol. 2508, no. 1, pp. 22–30, Jan. 2015, https://doi.org/10.3141/2508-03.

[13] S.-W. Yoo, G.-S. Ryu, and J. F. Choo, "Evaluation of the effects of high-volume fly ash on the flexural behavior of reinforced concrete beams," *Construction and Building Materials*, vol. 93, pp. 1132–1144, Sep. 2015, https://doi.org/10.1016/j.conbuildmat.2015.05.021.

[14] L. Zhou, P. Dong, Y. Zheng, G. Song, and X. Wang, "Investigation of the Structural Behaviors of One-way HVFA-SCC Slabs Reinforced by GFRP Bars," *Current Chinese Science*, vol. 1, no. 1, pp. 160–182, https://doi.org/10.2174/2210298101666200909160857.

[15] J. Dragaš, S. Marinković, I. Ignjatović, N. Tošić, and V. Koković, "Flexural behaviour and ultimate bending capacity of high-volume fly ash reinforced concrete beams," *Engineering Structures*, vol. 277, Feb. 2023, Art. no. 115446, https://doi.org/10.1016/j.engstruct.2022.115446.

[16] M. F. Falah, S. Kristiawan, and H. Saifullah, "Tension-Stiffening of Reinforced HVFA-SCC Beams," *Jordan Journal of Civil Engineering*, vol. 17, no. 3, pp. 497–512, Jul. 2023, https://doi.org/10.14525/JJCE.v17i3.11.

[17] *Building Code Requirements for Structural Concrete*. Farmington Hills, MI, USA: ACI, 2019.